

Exploring land surface temperature earthquake precursors: A focus on the Gujarat (India) earthquake of 2001

Blackett, M. , Wooster, M. and Malamud, B.

Published version deposited in CURVE February 2012

Original citation & hyperlink:

Blackett, M. , Wooster, M. and Malamud, B. (2011) Exploring land surface temperature earthquake precursors: A focus on the Gujarat (India) earthquake of 2001. Geophysical Research Letters, volume 38 (L15303).

<http://dx.doi.org/10.1029/2011GL048282>

Publisher statement: ©2011. American Geophysical Union. All Rights Reserved.

Copyright © and Moral Rights are retained by the author(s) and/ or other copyright owners. A copy can be downloaded for personal non-commercial research or study, without prior permission or charge. This item cannot be reproduced or quoted extensively from without first obtaining permission in writing from the copyright holder(s). The content must not be changed in any way or sold commercially in any format or medium without the formal permission of the copyright holders.

CURVE is the Institutional Repository for Coventry University

<http://curve.coventry.ac.uk/open>

1 Exploring land surface temperature earthquake precursors: 2 A focus on the Gujarat (India) earthquake of 2001

3 Matthew Blackett,^{1,2} Martin J. Wooster,¹ and Bruce D. Malamud¹

4 Received 27 May 2011; revised 13 June 2011; accepted 26 June 2011; published XX Month 2011.

5 [1] There are many reports of land surface temperature (LST) 23.41°N and 70.23°E) which killed over 20,000 people and 55
6 anomalies appearing prior to large earthquakes. A number of caused over US\$ 10 billion of damage [Mishra *et al.*, 2005; 56
7 methods have been applied in hindcast mode to identify National Earthquake Information Center, Preliminary earth- 57
8 these anomalies, using infrared datasets collected from quake report, 2004, available at <http://neic.usgs.gov/neis/> 58
9 Earth-orbiting remote sensing satellites. Here we examine eq_depot/2001/eq_010126/, accessed May 2011]. This event 59
10 three such methods and apply them to six years (2001–2006) has been subject to a number of hindcast studies claiming to 60
11 of MODIS LST data collected over the region of the 2001 have identified thermal precursory signals using various IR 61
12 Gujarat (India) earthquake, which previous studies have remote sensing datasets [Ouzounov and Freund, 2004; Saraf 62
13 identified as a site exhibiting possible pre-seismic and post- and Choudhury, 2005a; Genzano *et al.*, 2007]. 63
14 seismic thermal anomalies. Methods 1 and 2 use an LST
15 differencing technique, while Method 3, the Robust Satellite
16 Technique (RST), has been developed specifically for the
17 identification of thermal anomalies within spatio-temporal
18 datasets. In relation to the Gujarat Earthquake, results from
19 Methods 1 and 2 (LST differencing) indicate that changes
20 previously reported to be potential precursory thermal
21 ‘anomalies’ appear instead to occur within the range of
22 normal thermal variability. Results obtained with Method 3
23 (RST) do appear to show significant ‘anomalies’ around
24 the time of the earthquake, but we find these to be related
25 to positive biases caused by the presence of MODIS LST
26 data gaps, attributable to cloud cover and mosaicing of
27 neighboring orbits of data. Currently, therefore, we find no
28 convincing evidence of LST precursors to the 2001 Gujarat
29 earthquake, and urge care in the use of approaches aimed at
30 identifying such seismic thermal anomalies. **Citation:** Blackett, M.,
31 M. J. Wooster, and B. D. Malamud (2011), Exploring land surface
32 temperature earthquake precursors: A focus on the Gujarat (India)
33 earthquake of 2001, *Geophys. Res. Lett.*, 38, LXXXXX,
34 doi:10.1029/2011GL048282.

35 1. Introduction

36 [2] There is a long, sometimes controversial, history of 23.41°N and 70.23°E) which killed over 20,000 people and 55
37 research relating to earthquake precursors. Among such caused over US\$ 10 billion of damage [Mishra *et al.*, 2005; 56
38 studies, many relate to possible thermal anomalies seen prior National Earthquake Information Center, Preliminary earth- 57
39 to large seismic events [e.g., Wang and Zhou, 1984; Gornyy quake report, 2004, available at <http://neic.usgs.gov/neis/> 58
40 *et al.*, 1988; Qiang *et al.*, 1997; Panda *et al.*, 2007; Pergola eq_depot/2001/eq_010126/, accessed May 2011]. This event 59
41 *et al.*, 2010]. Here we further explore some approaches has been subject to a number of hindcast studies claiming to 60
42 used previously to identify ‘precursory thermal anomalies’ have identified thermal precursory signals using various IR 61
43 within infrared (IR) imagery taken from Earth-orbiting remote sensing datasets [Ouzounov and Freund, 2004; Saraf 62
44 satellites, in particular examining the methods’ sensitivities and Choudhury, 2005a; Genzano *et al.*, 2007]. 63
45 time series length and data gaps caused by incomplete records
46 and/or variations in cloudiness. We focus here on the $M_W =$
47 7.7 Gujarat (India) earthquake of 26 January 2001 (epicenter

¹Environmental Monitoring and Modelling Research Group, Department of Geography, King’s College London, London, UK.

²Now at Environment, Hazards and Risk Applied Research Group, Coventry University, Coventry, UK.

23.41°N and 70.23°E) which killed over 20,000 people and 55
caused over US\$ 10 billion of damage [Mishra *et al.*, 2005; 56
National Earthquake Information Center, Preliminary earth- 57
quake report, 2004, available at <http://neic.usgs.gov/neis/> 58
eq_depot/2001/eq_010126/, accessed May 2011]. This event 59
has been subject to a number of hindcast studies claiming to 60
have identified thermal precursory signals using various IR 61
remote sensing datasets [Ouzounov and Freund, 2004; Saraf 62
and Choudhury, 2005a; Genzano *et al.*, 2007]. 63

2. Background

[3] Early reports of possible air temperature variations 64
related to seismic activity are detailed by Milne [1886], but 65
the first attempts at measuring potential precursory Land 66
Surface Temperature (LST) phenomena did not appear until 67
the 1980s when, for example, Wang and Zhou [1984] claimed 68
to have identified soil temperature ‘anomalies’ prior to the 69
1976 Chinese Tangshan Earthquake. Gornyy *et al.* [1988] 70
went on to detail the use of satellite thermal infrared (TIR) 71
data in identifying similar phenomena in Central Asian 72
earthquake zones, and many subsequent works have also used 73
satellite TIR data [e.g., Genzano *et al.*, 2007; Pergola *et al.*, 74
2010]. Other studies report significant (4–10 K) pre-seismic 75
thermal anomalies across wide regions, based on analysis of 76
satellite-retrieved LST data derived from TIR observations 77
[e.g., Saraf and Choudhury, 2005b; Panda *et al.*, 2007]. 78
However, while informative in many ways, these studies 79
often appear limited in the quantity of data used to discrim- 80
inate ‘thermal anomalies’ from natural variability [e.g., 81
Ouzounov and Freund, 2004]. Furthermore, while some 82
studies use more advanced statistical techniques [e.g., 83
Genzano *et al.*, 2007; Panda *et al.*, 2007; Genzano *et al.*, 84
2009; Pergola *et al.*, 2010], the sensitivity of these approa- 85
ches to data gaps caused by cloud cover or other data cover- 86
age variations has not been fully assessed. Here we analyze 87
six full years (2001–2006) of daily MODIS LST data for the 88
Gujarat region of India. We explore the existence of LST 89
‘anomalies’ related to this event using this extended dataset, 90
along with analytical techniques based on those applied in 91
previous earthquake thermal precursor studies [e.g., 92
Ouzounov and Freund, 2004; Filizzola *et al.*, 2004; Genzano 93
et al., 2007]. 94
95

3. Dataset Description

[4] We used daily night-time LST data for the Gujarat 97
region, 2001–2006, extracted from the 1 km spatial reso- 98
lution gridded v.4 MOD11A1 LST product, which is itself 99
derived from TIR observations made by the MODIS 100
instrument operating on board the polar-orbiting Terra 101
spacecraft (detailed by Wan [1999]) (hereafter, MOD11A1). 102
During 2001–2006, besides the 26 January 2001 Gujarat 103

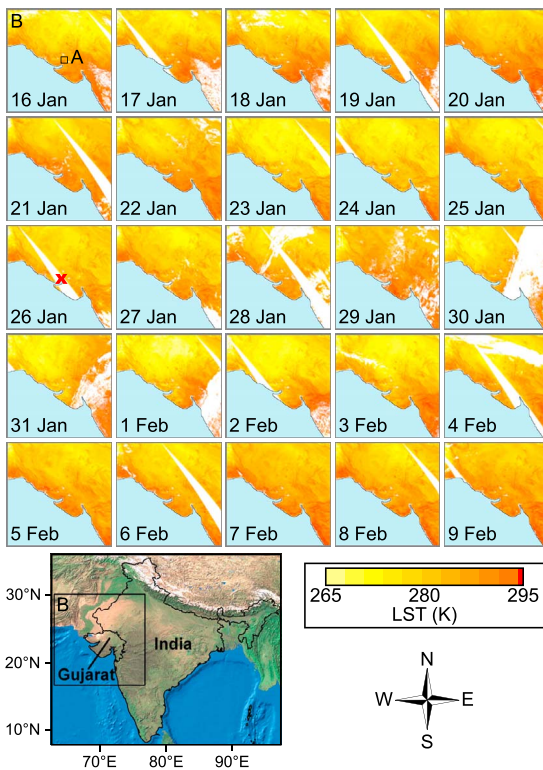


Figure 1. Night-time Land Surface Temperature (LST) maps for the Gujarat (India) region, 16 January–9 February 2001, with the 26 January 2001 Gujarat earthquake epicenter indicated by a red cross. Data are subset from the 1 km spatial resolution MODIS LST product (MOD11A1). This consists of data from the Terra MODIS sensor’s night-time overpass (~22:15 to ~23:15 Indian Standard Time). LST data for two regions are presented, each centered on the earthquake epicenter (23.41°N, 70.23°E): (i) Region A: 100 km × 100 km, boxed area highlighted in the 16 January LST map; (ii) Region B: 1500 km × 1500 km (each LST map’s total area). Region B is also boxed in the wider scale map at lower left (map source: ESRI, World Image.lyr, ArcGIS Software v. 10, Redlands, California, 1998). In each LST map, cloud cover and data gaps that remain between neighboring MODIS swaths are masked as white, while blue areas represent the Indian Ocean.

104 $M_W = 7.7$ earthquake, in a 750 km radius around Gujarat,
 105 there were no other similar-sized earthquakes (2nd largest
 106 earthquake, $M_W = 5.8$, 28 January 2001; two $M_W = 5.5$ in
 107 2006 (National Earthquake Information Center, US Geo-
 108 logical Survey earthquake database, 2011, available at
 109 <http://earthquake.usgs.gov/earthquakes/eqarchives/epic/>,
 110 accessed May 2011)).

111 [5] Two subsets of the Gujarat region were extracted for
 112 the six years of MOD11A1 data, both centered on the
 113 Gujarat earthquake epicenter: Region A (100 km × 100 km)
 114 formally examined by *Ouzounov and Freund* [2004], and a
 115 larger Region B (1500 km × 1500 km), representative of
 116 wider areas considered in other seismic thermal precursor
 117 studies [e.g., *Qiang et al.*, 1997; *Choudhury et al.*, 2006].
 118 Example LST data from 25 days (16 January–9 February
 119 2001) are shown in Figure 1 for Region B, with the smaller
 120 Region A shown boxed in the 16 January 2001 LST map. In
 121 these LST maps, light-blue represents the Indian Ocean
 122 (39.9% of 1500 × 1500 pixels in Region B).

[6] Each LST map (Figure 1) is derived from measure- 123
 ments of earth-emitted TIR spectral radiance made in MODIS 124
 bands 31 [11.00 μm] and 32 [12.02 μm], combined using the 125
 generalized split-window algorithm of *Wan and Dozier* 126
 [1996] and the land-cover classification-based emissivity 127
 approach of *Snyder et al.* [1998]. Cloudy pixels are masked 128
 using the methods of *Ackerman et al.* [2006]. To provide near 129
 complete spatial coverage on a daily basis, LST data derived 130
 from neighboring satellite orbits are mosaiced together in 131
 each MOD11A1 product file. Following this mosaicing 132
 process, areas with no useful LST data often remain in each 133
 product file due to cloud cover and gaps between the swaths 134
 of neighboring orbits, particularly at lower latitudes. In terms 135
 of accuracy, *Wolfe et al.* [2002] indicate that typical MODIS 136
 product geolocation precision is within 50 m (at nadir), and in 137
 a study focused on the Tibetan region, *Wang et al.* [2007] 138
 report that the MOD11A1 LST product displays a mean 139
 difference of 0.27 K when compared to *in situ* measures. 140

4. Methods 141

4.1. Data Processing 142

[7] Initial examining of the 1500 km × 1500 km Region B 143
 LST daily data, 2001–2006, found per-pixel LSTs as low as 144
 197 K. Analysis of corresponding MODIS Level 1b radiance 145
 products confirmed these as cloudy pixels undetected by the 146
Ackerman et al. [2006] tests. Using various LST minima 147
 thresholds, we remove these pixels, providing further ‘cloud 148
 screening’. Unusable land pixels are white in Figure 1. After 149
 pre-processing the 2190 daily MOD11A1 scenes available 150
 2001–2006, for Region A [B], 27% [17%] of scenes were 151
 classed unusable due to >75% of their land pixels having 152
 no usable LST data (cloud cover or mosaicing gaps); these 153
 scenes were removed from subsequent analysis. For Region A 154
 [B], the remaining 1601 [1820] scenes are used in our analyses, 155
 with 70% [89%] of the unusable scenes for Region A [B] 156
 occurring during the Indian Monsoon (June to September), and 157
 only 4% [1%] in the 5 January–16 February window (2001– 158
 2006) which in 2001 includes the Gujarat earthquake. All LST 159
 maps in Figure 1 (16 January–9 February 2001) are usable for 160
 Region B’s study, and only the 26 January (Gujarat earthquake 161
 date) was removed for Region A. 162

[8] The final six-year, cloud-screened LST dataset had three 163
 methods applied to test for “pre-seismic” thermal anomalies: 164

[9] 1. Method 1 — LST difference between the ‘earthquake’ 165
 year and one other year, as used by *Ouzounov and Freund* 166
 [2004]. 167

[10] 2. Method 2 — an extension of Method 1, based on 168
 the LST difference between each year of data (2001–2006) 169
 and the mean LST derived from all six years. 170

[11] 3. Method 3 — the Robust Satellite Technique (RST) 171
 statistical approach of *Tramutoli* [1998]. The RST was first 172
 developed for AVHRR thermal anomaly discrimination by 173
Tramutoli [1998], and most recently applied to MODIS data 174
 of the 2009 L’Aquila (Italy) earthquake [*Pergola et al.*, 2010]. 175

4.2. Method 1: LST Differencing (Based on Two Years) 176

[12] To test for potential thermal anomalies linked to the 177
 2001 Gujarat earthquake, *Ouzounov and Freund* [2004] 178
 calculated the spatially averaged daily mean MODIS LST 179
 of an area equivalent to Region A (Figure 1) for a number of 180
 weeks either side of the earthquake, and for the equivalent 181
 days of the year in 2002. They then calculated the difference 182

183 between the ‘earthquake’ and ‘non-earthquake’ year mea-
 184 surements ($\Delta LST_{2001-2002}$) for each day of the year (DOY),
 185 and identified what they termed a “thermal anomaly pattern”
 186 [Ouzounov and Freund, 2004, p. 269]. We reproduce this
 187 method for Region A (5 January–16 February) and then
 188 extend the method to all other pairs of years ΔLST_{a-b} , where
 189 $a \& b = (2001, 2002, \dots, 2006, a \neq b)$, i.e. up to 30 com-
 190 binations per ‘day’.

191 4.3. Method 2: Extended LST Differencing 192 (Based on Multiple Years)

193 [13] Method 1 differences two years of data (a and b), so
 194 that the resulting measure (ΔLST_{a-b}) is as much influenced
 195 by b (the ‘baseline’ year) as by a (the year of interest). To
 196 mitigate this influence, we repeat the approach of Ouzounov
 197 and Freund [2004] using Region A data, but extend it by
 198 deriving a ‘climatological average’ LST to which 2001
 199 could be independently compared. We then applied the
 200 same procedure to all six years, calculating the spatially
 201 averaged mean LST for each DOY (d) for each year (2001,
 202 2002, ..., 2006), Region A, giving $LST_A(d)_{year}$. Then, for
 203 a given DOY, up to six values are available (2001, 2002,
 204 ..., 2006); these were averaged to provide ‘climatological’
 205 mean DOY values ($\overline{LST_A}(d)$) which were subtracted from
 206 the respective daily (d) values ($LST_A(d)_{year}$). This quanti-
 207 fies the LST difference between the date of interest and the
 208 corresponding six-year mean ($\Delta LST_{A,year}$). We take $\Delta LST_{A,$
 209 $year$ as our ‘anomaly’ measure, with up to 6 values for a
 210 given day of year.

211 4.4. Method 3: Robust Satellite Technique (RST)

212 [14] A detailed description of the RST as applied to
 213 remotely sensed LST data is given by Filizzola et al. [2004].
 214 In summary, the technique functions by comparing the LST
 215 for a particular pixel and DOY (LST_r) to both the spatial
 216 mean of that particular scene ($LST_A(d)_{year}$ and LST_B
 217 $(d)_{year}$, Regions A and B respectively) and to the temporal
 218 mean (over multiple years considered) of LST for that
 219 particular pixel and DOY ($\overline{LST_r}$). This is normalized by the
 220 standard deviation (again, over multiple years) of the LST
 221 values for that particular pixel and DOY ($\sigma [LST_r]$). The aim
 222 is to provide a method of isolating pixels whose LST signal
 223 appears thermally anomalous when compared with the
 224 longer-term local spatial average [Tramutoli, 2007].

225 [15] Application of the RST results in the derivation of an
 226 index value (R_I) for each pixel (here given for Region A):
 227 $R_I = \{LST_r - LST_A(d)_{year} - \overline{LST_r}\} / \sigma [LST_r]$, where R_I
 228 represents the LST departure from the spatio-temporal his-
 229 torical ‘average’, weighted by its historical variability
 230 [Genzano et al., 2009]. This index value is derived from the
 231 more general *Absolutely Local Index of Change of the*
 232 *Environment* (ALICE) of Tramutoli [1998]. When applied
 233 to seismic monitoring it is often referred to as the *Robust*
 234 *Estimator of TIR Anomalies* (RETIRA) [Tramutoli et al.,
 235 2005; Aliano et al., 2008a]. For a specific year, the
 236 RETIRA index value (R_I) for a given pixel and day can be
 237 interpreted as the number of standard deviations its LST
 238 (LST_r) is from that pixel’s mean ($\overline{LST_r}$) for that DOY, over
 239 all years considered, adjusted for each scene’s spatial mean.

240 [16] Aliano et al. [2008a] suggested that the RST can, in
 241 some cases, be impacted by the presence of cloud-related
 242 data ‘gaps’. We explored and confirmed this using a set of

LST simulations (see auxiliary material).¹ Despite potential
 bias in the RETIRA index caused by cloud-cover variations
 or other data gaps, use of the RST has continued in seismic
 thermal precursor studies [e.g., Aliano et al., 2008b;
 Genzano et al., 2009; Pergola et al., 2010].

[17] We applied the RST to the six-year (2001–2006)
 MODIS LST dataset of Region A, so as to further examine
 the data at the scale used by Ouzounov and Freund [2004].
 We then, as have other studies [e.g., Qiang et al., 1997;
 Choudhury et al., 2006; Genzano et al., 2007], applied the
 RST to a much larger region (Region B). In these applica-
 tions the six-year mean and standard deviation for each
 MOD11A1 pixel and DOY ($\overline{LST_r}$ and $\sigma [LST_r]$, respec-
 tively), were calculated using a 15-day moving window of
 LST data, centered on the DOY in question. This ensured
 that even during persistent cloud cover or other data gaps, a
 significant number of observations (up to 15 per DOY for
 each of the six years, or 90 values) contributed to calculating
 $\overline{LST_r}$ and $\sigma [LST_r]$ for each pixel.

[18] Here, we take the number of pixels (N_A and N_B)
 exceeding a selected R_I threshold in Regions A and B,
 respectively, as a measure of the degree to which the
 MOD11A1 data of a particular date contains LST ‘anoma-
 lies’; N_A and N_B are expressed as a percentage of the total
 number of useable land pixels within the scene (*Percentage*
 N_A and *Percentage* N_B , respectively). In previous studies,
 R_I values have been classified as ‘anomalous’ using various
 thresholds, for example: >2.0 , >2.5 , >3.0 and >3.5
 [Tramutoli et al., 2005]; ≥ 2.0 and ≥ 3.0 [Genzano et al.,
 2007]; and ≥ 2.0 , ≥ 2.5 and ≥ 3 [Pergola et al., 2010]. We
 found that over all DOY considered (2001–2006), the per-
 centage of ‘anomalous’ pixels for different thresholds was
 for Region A [B]: $R_I \geq 2.0$ (2.27% [1.44%]), $R_I \geq 2.5$ (0.62%
 [0.29%]), and $R_I \geq 3.0$ (0.13% [0.06%]). We use $R_I \geq 2.5$ to
 represent ‘anomalous’ pixels.

278 5. Results

279 5.1. Method 1: LST Differencing (Based on Two Years)

[19] Figure 2a shows ΔLST_{a-b} derived using Method 1 as
 a function of DOY for Region A, 5 January–16 February,
 i.e. 26-days including the 26 January 2001 Gujarat earth-
 quake date. The dotted line gives our reproduction of the
 Ouzounov and Freund [2004] $\Delta LST_{2001-2002}$ time series,
 where spatially averaged LST data from the same DOY in
 2001 and 2002 are differenced. Extended to all six years
 (2001–2006), the envelopes are the maximum (pink) and
 minimum (blue) daily values for ΔLST_{a-b} , with $a \& b =$
 (2001, 2002, ..., 2006). The dotted line ($\Delta LST_{2001-2002}$)
 shows a large local peak five days prior to the 26 January
 earthquake, as originally indicated by Ouzounov and Freund
 [2004], but compared against the backdrop of all the other
 years this peak no longer appears anomalous, with the upper
 envelope showing eight peaks of greater magnitude in this
 relatively short period of the year.

296 5.2. Method 2: Extended LST Differencing 297 (Based on Multiple Years)

[20] Figure 2b shows the results of ‘extended’ LST
 differencing, where for each of the 26 days (5 January–
 299

¹Auxiliary materials are available in the HTML. doi:10.1029/2011GL048282.

300 16 February) we use six years of data (2001–2006) to cal-
 301 culate the mean LST to compare with each scene’s LST
 302 (vs. just one year compared to another in Method 1). The
 303 dashed line shows our $\Delta LST_{A,2001}$ measure (section 4.2).
 304 Around the period of the 26 January earthquake, $\Delta LST_{A,2001}$
 305 shows a similar pattern to that of the *Ouzounov and Freund*
 306 [2004] $\Delta LST_{2001-2002}$ time series (Figure 2a), both im-
 307 mediately prior to (and to some extent also subsequent to) the
 308 earthquake event itself.
 309 [21] However, when we calculate $\Delta LST_{A,year}$, but this
 310 time substitute 2001, 2002, ..., 2006, for the *year* being
 311 analyzed, as we found in Figure 2a, both comparable and
 312 larger peaks are actually seen in all other years (Figure 2b).
 313 The outer envelope of Figure 2b shows the maximum and
 314 minimum extent of $\Delta LST_{A,year}$ for each DOY (2001–2006),
 315 while Figure S1 in the auxiliary material shows the annually

calculated measures used to construct this envelope. The 316
 envelope in Figure 2b indicates that the pre-event (and 317
 indeed post-event) LST peaks seen by *Ouzounov and* 318
Freund [2004], and in our similar $\Delta LST_{A,2001}$ measure, 319
 although seemingly anomalous for this period in 2001, are 320
 not unusual when seen against $\Delta LST_{A,year}$ calculated for all 321
 six years. In particular, the $\Delta LST_{A,2001}$ peaks surrounding 322
 26 January occur within the envelope of values found 323
 throughout the six-year period. 324

5.3. Method 3: Robust Satellite Technique (RST) 325

[22] Following the removal of scenes containing very 326
 significantly incomplete LST records in Region A [B] (see 327
 section 4.1), we now apply the RST (Method 3, described in 328
 section 4.3) to the remaining 1601 [1820] LST scenes for 329
 Region A [B]. We examine values of the RETIRA index, R_I , 330
 for each DOY. In applying the RST to our Region A [B] 331
 dataset, the number of scenes displaying 0 pixels with R_I 332
 ≥ 2.5 was 42% [15%]. For each of the 1601 Region A LST 333
 scenes, after calculating R_I using all useable land pixels, the 334
 probability of a given value of R_I occurring was calculated. 335

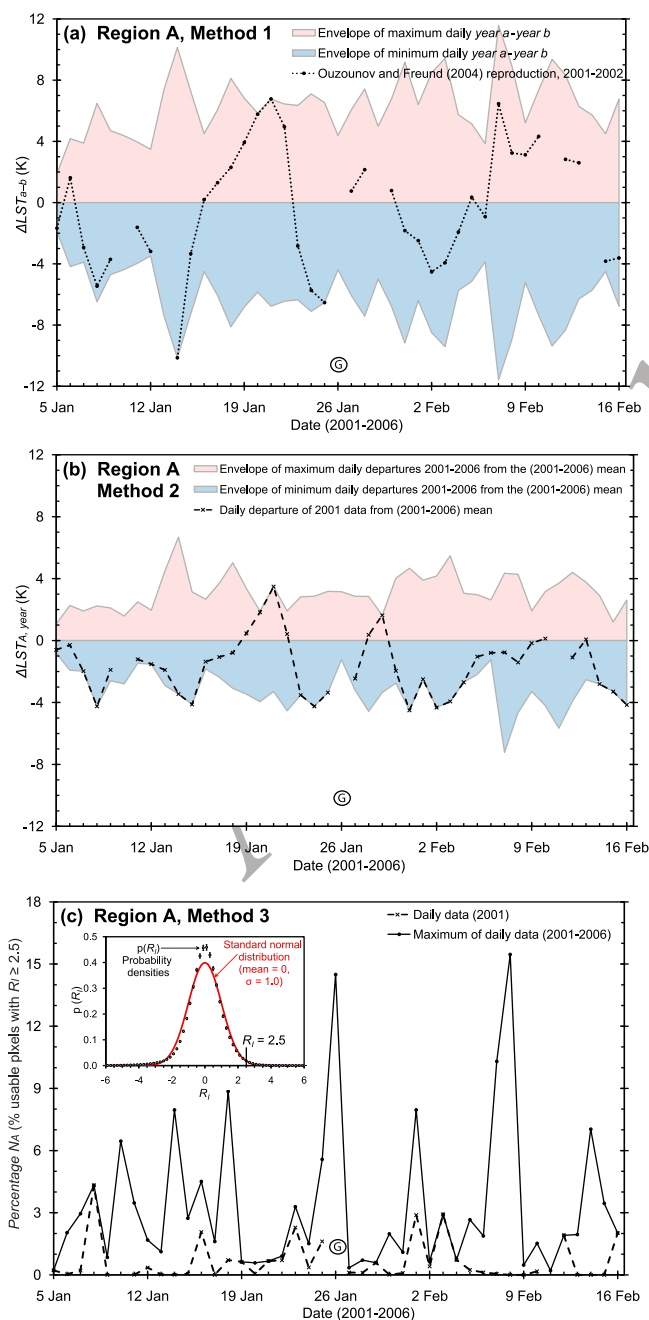


Figure 2. Land Surface Temperature (LST) differencing techniques, and Robust Satellite Technique (RST), applied to Region A (see Figure 1) for 5 January–16 February, 2001–2006. LST data were derived for each DOY (2001–2006) in the period surrounding the 26 January 2001 Gujarat earthquake, extracted from the 1 km spatial resolution MOD11A1 product for Region A (see Figure 1): (a) LST difference (two individual years) calculated as described in section 4.2 (Method 1) with the difference in Region A mean LST for a particular DOY (d) and year ($LST_A(d)_{year}$) calculated between years a and b , (ΔLST_{a-b}); a & $b = (2001, 2002, \dots, 2006, a \neq b)$. The envelope of maximum (pink) and minimum (blue) daily values is shown for each DOY. The dotted black line ($\Delta LST_{2001-2002}$) is our reproduction of *Ouzounov and Freund* [2004] for the ‘earthquake’ year 2001 and the ‘non-earthquake’ 2002. (b) LST difference (multiple years) calculated as described in section 4.3 (Method 2). For a given day of year (d), the spatial average of LST for Region A in each of the six years was calculated ($LST_A(d)_{year}$) and averaged to provide $LST_A(d)$. The dashed line is the daily departure from $LST_A(d)$ for the 2001 earthquake year, i.e. $\Delta LST_{A,2001} = LST_A(d)_{2001} - LST_A(d)$. The colored envelope represents the daily maxima and minima of $\Delta LST_{A,year}$ calculated from data considering each of the six years (2001–2006) individually. (c) RETIRA index (R_I) values calculated using the RST [Tramutoli, 1998] as described in section 4.3 (Method 3). The dashed line shows the percentage of usable pixels with $R_I \geq 2.5$ (Percentage N_A) for 2001, while the solid line is the daily maxima of Percentage N_A for all six years, 5 January–16 February. The inset shows the average probability densities (± 1 standard error) of R_I pixel values, for all 1601 usable scenes available over the six years, along with a standard normal distribution (red line, mean 0, standard deviation $\sigma = 1.0$). Thresholds of $R_I \geq 2.0$, 2.5 and 3.0 represent 2.27% (2σ), 0.62% (2.5σ), 0.13% (3σ), respectively, of the values in the probability density distribution. In Figures 2a–2c, breaks in the record are due to the removal of scenes with $>75\%$ of land pixels having no usable LST data. The Gujarat earthquake date (26 January 2001) is represented as a circled ‘G’.

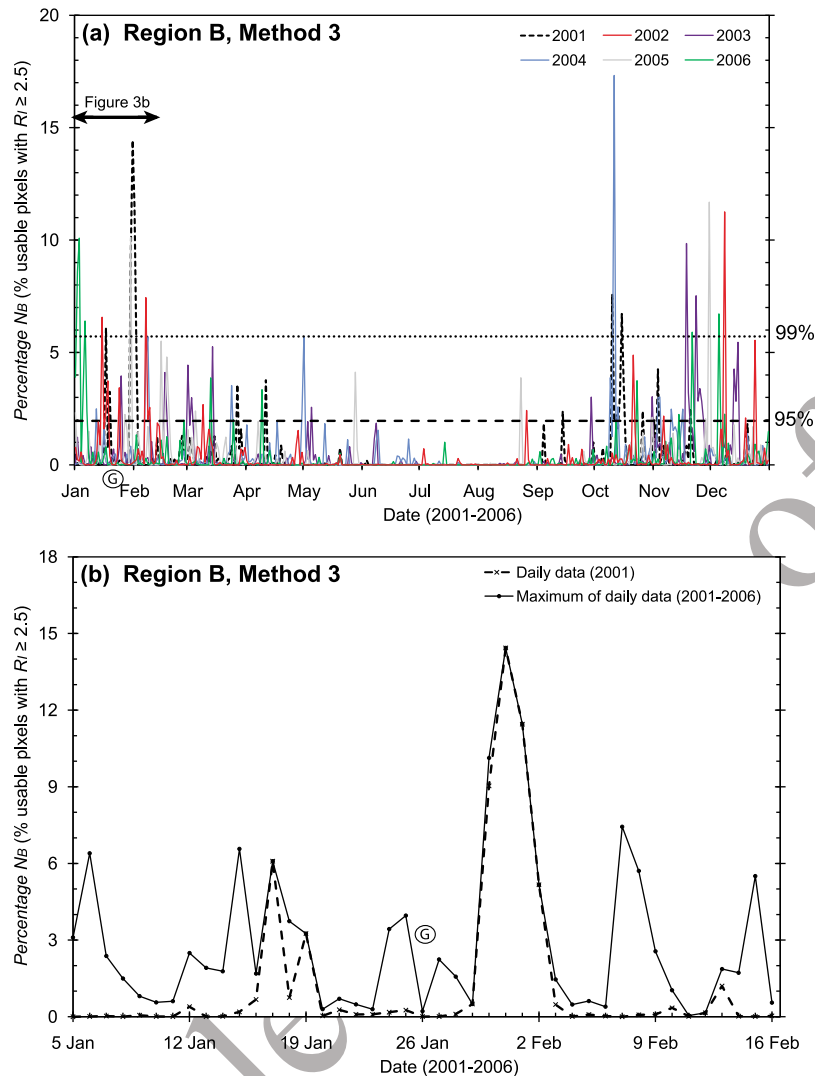


Figure 3. The Robust Satellite Technique (RST, Method 3) applied to daily MODIS LST data, 2001–2006, for a 1500 km × 1500 km area surrounding Gujarat, India. LST data were extracted from the 1 km spatial resolution v.4 MOD11A1 product for Region B (area covered by Figure 1 LST maps). Periods considered are (a) all days in the year, and (b) the six weeks (1 January–16 February) surrounding the date of the 26 January 2001 Gujarat earthquake. On the y-axis for Figures 3a and 3b is *Percentage N_B*, the percentage of usable pixels within the scene having RETIRA index [Tramutoli *et al.*, 2005] (see section 4.3) $R_I \geq 2.5$. The threshold of $R_I \geq 2.5$ represents the upper 0.29% of the probability density distribution of all R_I values for all usable scenes of the six year period (1820 scenes). The dashed black time series line for Figures 3a and 3b shows *Percentage N_B* for 2001, with each colored line in Figure 3a representing *Percentage N_B* for each of the six years, and the solid line in Figure 3b the daily maxima of *Percentage N_B* for all six years. In Figure 3a we use the 1820 scenes that remained following the removal of unusable scenes (i.e., those having data gaps covering >75% of land pixels). The horizontal dashed and dotted lines represent the 95th and 99th percentiles of *Percentage N_B* respectively. The Gujarat earthquake date (26 January 2001) is represented as a circled ‘G’.

336 In Figure 2c (inset graph), $p(R_I)$, the average probability
 337 density at a given R_I , is given over the range $-6 \leq R_I \leq 6$. The
 338 average probability densities of our ‘real’ data are reasonably
 339 similar to a standard Gaussian distribution (solid curve,
 340 Figure 2c, inset graph), i.e. mean 0, standard deviation 1.0.
 341 [23] In Figure 2c we also present the *Percentage N_A*
 342 (percentage of useable land pixels with $R_I \geq 2.5$) in Region
 343 A as a function of DOY, 5 January–16 February. The
 344 dashed line shows the results for 2001 and the solid thin line
 345 the maximum of daily data for 2001–2006. The 2001 data
 346 (dashed line) shows a small peak (23 January) before the
 347 earthquake event in 2001, although offset slightly tempo-

rally in relation to the ‘precursory LST peak’ of Figure 2b. 348
 However, examination of maximum *Percentage N_A* data for 349
 all other years (solid line, Figure 2c) reveals many more 350
 peaks at other times, so we see no evidence for ‘seismic 351
 thermal precursors’ at the Region A scale. 352

[24] Figure 3a presents *Percentage N_B* (% of usable land 353
 pixels with $R_I \geq 2.5$) at the Region B scale, for every DOY 354
 (1–365), and year (2001–2006). It shows for 2001 (dashed 355
 line) large ‘pre-seismic’, and in particular ‘post-seismic’ 356
 peaks in *Percentage N_B*. Figure 3b focuses on 5 January– 357
 16 February, the ‘earthquake period’, and shows that for 358
 2001, peaks around 17 and 19 January (pre-seismic) and 359

360 30 January–2 February (post-seismic), are the largest on
 361 those particular DOYs in the entire six years. Indeed, the
 362 post-seismic peak is the second-largest of the six-year
 363 period (Figure 2a), and both ‘pre-’ and ‘post-seismic’ peaks
 364 fall within the upper 1% of *Percentage N_B* values of all 1820
 365 scenes for this dataset.

366 [25] Re-inspection of Figure 1 however, confirms that
 367 daily LST data coverage for Region B has varying degrees
 368 of completeness due to cloud cover and mosaicing gaps. For
 369 example, on the 16, 20, 30 January 2001, 11%, 3%, and
 370 41% respectively of the land in Region B has no usable LST
 371 data. In particular, there are days (Figure 1) when substantial
 372 areas towards the south-east of Region B have no usable
 373 LST data (17–19 January and 30 January–2 February). With
 374 clear skies, the south-east exhibits the highest LSTs of the
 375 region, as confirmed when the spatial mean LST of the area
 376 covered by cloud on 30 January 2001 (283.5 K; standard
 377 deviation, $\sigma = 1.5$ K) is compared to that of the remaining
 378 cloud free surface for the period represented (281.7 K; $\sigma =$
 379 1.8 K). The absence of data for this usually warmer region
 380 between 30 January and 2 February reduces the scene-wide
 381 LST mean ($LST_B(d)_{year}$) for those dates, thereby lowering
 382 the LST required for any particular pixel to display $R_I \geq 2.5$
 383 and producing the corresponding *Percentage N_B* peak
 384 (Figure 3b). The smaller, but still significant data gaps over
 385 this warmer south-east region around 17–19 January cor-
 386 respond with the smaller ‘pre-cursory’ *Percentage N_B* peak
 387 (Figure 3b). The magnitude of these peaks is subdued when
 388 higher R_I thresholds (i.e. $R_I \geq 3.0$ and $R_I \geq 3.5$) are applied,
 389 but so too is that of all other peaks, confirming that altering
 390 R_I thresholds fails to eliminate the bias caused by data gaps
 391 that mask normally warmer areas of the study region.

392 [26] The cause of these effects is a direct result of the
 393 mean LST of the scene being lowered due to some of the
 394 normally warmer area being unobserved and thus removed
 395 from the calculation, resulting in pixels with lower LSTs
 396 than would otherwise be the case appearing ‘anomalous’
 397 based on R_I thresholding. The reverse happens when cloud
 398 masks a normally cooler region, and similarly there is little
 399 effect when cloud covers areas whose temperature is close
 400 to the scene average. Evidently cloud cover, and its precise
 401 location, can introduce significant bias into RST perfor-
 402 mance. We further explore and confirm this using simula-
 403 tions (Figures S2 and S3 in the auxiliary material).

404 6. Discussion and Conclusion

405 [27] The process of identifying potential thermal anoma-
 406 lies from within LST datasets requires the determination of
 407 ‘baseline’ conditions against which potential anomalies can
 408 be assessed. In general, the greater the number of years used
 409 to derive the measure of LST ‘natural variability’, the
 410 stronger can be the claim for any subsequent thermal
 411 anomaly identification. Here, for the 2001 Gujarat Earth-
 412 quake, we have used up to six years of MODIS LST data to
 413 calculate the baseline from which LST departures are ana-
 414 lyzed. We find that claims of seismic thermal precursors
 415 based on differencing only two years of data cannot be
 416 confirmed when we take into account the variability seen
 417 within a longer time series. Furthermore, we have shown
 418 that a more statistically-based method of thermal anomaly
 419 discrimination, the RST of *Tramutoli* [1998], can be sig-
 420 nificantly affected by positive biases when cloud cover or

other data gaps affect normally warmer scene areas. We
 suppose that such effects could be responsible for at least
 some of the reports of seismic thermal precursors that have
 been noted, not just in the case of Gujarat [e.g., *Genzano*
et al., 2007], but also in other studies that have isolated
 these using the RST [e.g., *Tramutoli et al.*, 2005; *Pergola*
et al., 2010].

[28] In an attempt to potentially account for such effects
 when using the RST, *Genzano et al.* [2009] and *Pergola*
et al. [2010] did remove remote sensing scenes displaying
 >80% cloud cover from their time series datasets. However,
 this would not have removed scenes such as that of 30
 January 2001 examined here — which had no usable LST
 data for 41% of the Region B land surface pixels due to
 cloud-cover and swath-related data gaps — and which
 resulted in a significant peak in the percentage of pixels
 showing elevated RETIRA index values (Figure 3b). Evi-
 dently, if biases are to be avoided the precise location of
 cloud, in addition to its areal coverage, must be considered
 when the RST is applied. Based on our findings, we con-
 clude that at present there is no robust evidence for the
 existence of LST anomalies prior to the 2001 Gujarat
 earthquake, and that reports of such precursory signals
 should be regarded cautiously until further instances of the
 phenomena become evident that stand up to detailed sta-
 tistical scrutiny.

447 Notation

$LST_A(d)_{year}$	spatial LST mean for a particular region (A), DOY (d) and year ($year$) (K).	449
$\overline{LST_A(d)}$	mean $LST_A(d)_{year}$ calculated using up to six years of data (K).	450–452
$\Delta LST_{A,year}$	the difference between $LST_A(d)_{year}$ and $\overline{LST_A(d)}$ (K).	453–454
ΔLST_{a-b}	difference in mean LST for a particular DOY year between two years a and b .	455–456
$\frac{LST_r}{LST_r}$	LST for a particular pixel and DOY (K). mean LST for a particular pixel calculated using up to six years of data (K).	457–459
R_I	RETIRA index value (unitless).	460
N_A	number of pixels with $R_I > 2.5$ for a particular region (A).	461–462

[29] **Acknowledgments.** This work was supported by an SSPP PhD
 grant, King’s College London. We thank NASA’s Land Processes Distribu-
 ted Active Archive Center (DAAC) for the data used in this study, and
 Stuart Gill (Coventry University) who assisted in cartography work.

467 References

- Ackerman, S. A., K. I. Strabala, W. P. Menzel, R. A. Frey, C. C. Moeller,
 L. E. Gumley, B. A. Baum, S. Wetzel Seeman and H. Zhang (2006), Dis-
 criminating clear-sky from cloud with MODIS, Algorithm Theoretical
 Basis Document, ATBD MOD35, version 5.0, NASA Goddard Space
 Flight Cent., Greenbelt, Md.
 Aliano, C., R. Corrado, C. Filizzola, N. Genzano, N. Pergola, and V. Tramutoli
 (2008a), Robust TIR satellite techniques for monitoring earthquake active
 regions: Limits, main achievements and perspectives, *Ann. Geophys.*, *51*,
 303–318.
 Aliano, C., R. Corrado, C. Filizzola, N. Pergola, and V. Tramutoli (2008b),
 Robust satellite techniques (RST) for the thermal monitoring of earth-
 quake prone areas: The case of Umbria-Marche October, 1997 seismic
 events, *Ann. Geophys.*, *51*, 451–459.
 Choudhury, S., S. Dasgupta, A. Saraf, and S. Panda (2006), Remote sens-
 ing observations of pre-earthquake thermal anomalies in Iran, *Int. J.*
Remote Sens., *27*, 4381–4396, doi:10.1080/01431160600851827.
 Filizzola, C., N. Pergola, C. Piertraposa, and V. Tramutoli (2004), Robust
 satellite techniques for seismically active areas monitoring: A sensitivity

- 486 analysis on September 7, 1999 Athens's earthquake, *Phys. Chem. Earth*,
487 29, 517–527.
- 488 Genzano, N., C. Aliano, C. Filizzola, N. Pergola, and V. Tramutoli (2007),
489 A robust satellite technique for monitoring seismically active areas: The
490 case of Bhuj–Gujarat earthquake, *Tectonophysics*, 431, 197–210,
491 doi:10.1016/j.tecto.2006.04.024.
- 492 Genzano, N., C. Aliano, R. Corrado, C. Filizzola, M. Lisi, G. Mazzeo,
493 R. Paciello, N. Pergola, and V. Tramutoli (2009), RST analysis of MSG–
494 SEVIRI TIR radiances at the time of the Abruzzo 6 April 2009 earthquake,
495 *Nat. Hazards Earth Syst. Sci.*, 9, 2073–2084, doi:10.5194/nhess-9-2073-
496 2009.
- 497 Gornyy, V., A. G. Sal'man, A. A. Tronin, and B. V. Shilin (1988), Outgoing
498 terrestrial infrared radiation as an indicator of seismic activity (in Russian),
499 *Dokl. Akad. Nauk USSR*, 301, 67–69.
- 500 Milne, J. (1886), *Earthquakes and Other Earth Movements*, D. Appleton,
501 New York.
- 502 Mishra, D. C., C. V. Chandrasekhar, and B. Singh (2005), Tectonics and
503 crustal structures related to Bhuj earthquake of January 26, 2001: Based
504 on gravity and magnetic surveys constrained from seismic and seismo-
505 logical studies, *Tectonophysics*, 396, 195–207, doi:10.1016/j.tecto.
506 2004.12.007.
- 507 Ouzounov, D., and F. Freund (2004), Mid-infrared emission prior to strong earth-
508 quakes analyzed by remote sensing data, *Adv. Space Res.*, 33, 268–273,
509 doi:10.1016/S0273-1177(03)00486-1.
- 510 Panda, S. K., S. Choudhury, A. K. Saraf, and J. D. Das (2007), MODIS
511 land surface temperature data detects thermal anomaly preceding 8 Octo-
512 ber 2005 Kashmir earthquake, *Int. J. Remote Sens.*, 28, 4587–4596,
513 doi:10.1080/01431160701244906.
- 514 Pergola, N., C. Aliano, I. Coviello, C. Filizzola, N. Genzano, T. Lacava,
515 M. Lisi, G. Mazzeo, and V. Tramutoli (2010), Using RST approach and
516 EOS-MODIS radiances for monitoring seismically active regions: A study
517 on the 6 April 2009 Abruzzo earthquake, *Hazards Earth Syst. Sci.*, 10,
518 239–249, doi:10.5194/nhess-10-239-2010.
- 519 Qiang, Z., X. Xu, and C. Dian (1997), Case 27: Thermal infrared anomaly pre-
520 cursor of impending earthquakes, *Pure Appl. Geophys.*, 149, 159–171,
521 doi:10.1007/BF00945166.
- 522 Saraf, A. K., and S. Choudhury (2005a), NOAA-AVHRR detects thermal
523 anomaly associated with the 26 January, 2001 Bhuj earthquake, Gujarat,
524 India, *Int. J. Remote Sens.*, 26, 1065–1073, doi:10.1080/
525 01431160310001642368.
- 526 Saraf, A. K., and S. Choudhury (2005b), Satellite detects surface thermal
527 anomalies associated with the Algerian earthquakes of May 2003, *Int.*
528 *J. Remote Sens.*, 26, 2705–2713, doi:10.1080/01431160310001642359.
- Snyder, W., Z. Wan, Y. Zhang, and Z. Feng (1998), Classification-based
emissivity for land surface temperature measurement from space, *Int.*
J. Remote Sens., 19, 2753–2774, doi:10.1080/014311698214497.
- Tramutoli, V. (1998), Robust AVHRR techniques (RAT) for environmental
monitoring: Theory and applications, in *Earth Surface Remote Sensing*
II, edited by G. Cecchi and E. Zilioli, *Proc. SPIE*, 3496, 101–113.
- Tramutoli, V. (2007), Robust satellite techniques (RST) for natural and
environmental hazards monitoring and mitigation: Theory and applica-
tions, in *Proceedings of Multi Temp 2007*, pp. 1–6, Inst. of Electr. and
Electron. Eng., New York, doi:10.1109/MULTITEMP.2007.4293057.
- Tramutoli, V., V. Cuomo, B. Filizzola, N. Pergola, and C. Piertraposa
(2005), Assessing the potential of thermal infrared satellite surveys for
monitoring seismically active areas: The case of Kocaeli (Izmit) earth-
quake, August 17, 1999, *Remote Sens. Environ.*, 96, 409–426,
doi:10.1016/j.rse.2005.04.006.
- Wan, Z. (1999), MODIS land surface temperature, Algorithm Theoretical
Basis Document (LST ATBD), version 3.3, NASA Goddard Space
Flight Cent., Greenbelt, Md.
- Wan, Z., and J. Dozier (1996), A generalized split-window algorithm for
retrieving land surface temperature from space, *IEEE Trans. Geosci.*
Remote Sens., 34, 892–905.
- Wang, K., Z. Wan, P. Wang, M. Sparrow, J. Liu, and S. Haginoya (2007),
Evaluation and improvement of the MODIS land surface temperature/
emissivity products using ground-based measurements at a semi-desert
site on the western Tibetan Plateau, *Int. J. Remote Sens.*, 28, 2549–2565,
doi:10.1080/01431160600702665.
- Wang, L., and C. Zhou (1984), Anomalous variations of ground temperature
before the Tangsan and Haiheng earthquakes (in Chinese), *J. Seismol.*
Res., 7, 649–656.
- Wolfe, R., M. Nishihama, A. Fleig, J. Kuyper, D. Roy, C. Storey, and F. Patt
(2002), Achieving sub-pixel geolocation accuracy in support of MODIS
land science, *Remote Sens. Environ.*, 83, 31–49, doi:10.1016/S0034-
4257(02)00085-8.
- M. Blackett, Environment, Hazards and Risk Applied Research Group,
Coventry University, Coventry CV1 5FB, UK. (matthew.blackett@
coventry.ac.uk)
- B. D. Malamud and M. J. Wooster, Environmental Monitoring and
Modelling Research Group, Department of Geography, King's College
London, London WC2R 2LS, UK.